Supporting Information

Efficient luminescence sensing in two lanthanide metal-organic frameworks with rich uncoordinated Lewis basic sites

Liming Deng, [a,b] Huihui Zhao, [a] Kang Liu, [a] and Dingxuan Ma, *[a]

[a] *Taishan Scholar Advantage and Characteristic Discipline Team of Eco Chemical Process and Technology, Key Laboratory of Eco-chemical Engineering, Qingdao University of Science and Technology, Qingdao 266042, P. R. China.*
[b] *Jiangsu Key Laboratory of Electrochemical Energy Storage Technologies, College of Materials Science and Technology, Nanjing University of Aeronautics and Astronautics, Nanjing 210016, P.R. China*
** Corresponding author.*
E-mail addresses: madingxuan640@126.com (D.X. Ma).

Table S1. Crystal date and structure refinement of **Eu-DTA** and **Tb-DTA**.

	Eu-DTA	**Tb-DTA**
Chemical formula	$\{[Eu(DTA)_{1.5}(H_2O)]\cdot H_2O\}_n$	$[Tb(DTA)(C_2O_4)_{0.5}(H_2O)]_n$
Empirical formula	$C_{21}H_{15}N_6O_8Eu$	$C_{15}H_{10}N_4O_7Tb$
Formula weight	631.35	517.19
T (K)	293(2)	293(2)
Crystal system	triclinic	triclinic
Space group	*P*Error!	*P*Error!
a (Å)	9.9901(8)	8.2132(5)
b (Å)	10.1477(7)	9.9550(7)
c (Å)	11.9438(9)	11.4034(6)
α (°)	64.998(7)	101.681(5)
β (°)	76.806(7)	102.242(5)
γ (°)	82.831(6)	107.250(6)
V (Å^3)	1067.85(15)	834.27(10)
Z	2	2
D_c (mg·mm^{-3})	1.964	2.059
μ (mm^{-1})	3.002	4.287
F(000)	620.0	498.0
Index ranges (h, k, l)	-13/13, -13/14, -16 /14	-9/9, -10/11, -13 /12
Reflections collected	8795	5814
R(int)	0.0482	0.0343
Data/Restraints/Parameters	5152/0/329	2945/0/249
GOF (F^2)	0.976	1.076
R_1, wR_2 [$I \geq 2\sigma(I)$]	0.0364, 0.0696	0.0322, 0.0716
R_1, wR_2 (all date)	0.0460, 0.0739	0.0382, 0.0751
Largest diff. peak and hole/ e Å^{-3}	1.43/-1.09	1.20/-0.81

$R_1 = \Sigma||F_o| - |F_c||/\Sigma|F_o|$. $wR_2 = [\Sigma w(|F_o^2| - |F_c^2|)^2 / \Sigma w|F_o^2|^2]^{1/2}$.

Table S2. Selected bond lengths (Å) and angles (°) for **Eu-DTA** and **Tb-DTA**.

Eu-DTA

Eu1-O1	2.475(3)	Eu1-O5	2.334(3)
Eu1-O2	2.395(2)	Eu1-O6	2.542(3)
Eu1-O3	2.359(3)	Eu1-O7	2.443(3)
Eu1-O4	2.379(3)	Eu1-N1	2.508(4)
O1-Eu1-O6	129.91(10)	O4-Eu1-O1	79.84(11)
O1-Eu1-N1	72.29(12)	O4-Eu1-O2	154.63(11)
O2-Eu1-O1	87.34(10)	O4-Eu1-O6	80.24(10)
O2-Eu1-O6	124.18(9)	O4-Eu1-O7	131.82(11)
O2-Eu1-O7	71.89(10)	O4-Eu1-N1	77.90(11)
O2-Eu1-N1	77.38(10)	O5-Eu1-O1	68.83(12)
O3-Eu1-O1	144.27(11)	O5-Eu1-O2	96.19(10)
O3-Eu1-O2	97.49(10)	O5-Eu1-O3	144.53(12)
O3-Eu1-O4	81.14(10)	O5-Eu1-O4	99.38(10)
O3-Eu1-O6	75.40(10)	O5-Eu1-O6	69.83(11)
O3-Eu1-O7	79.50(11)	O5-Eu1-O7	73.96(11)
O3-Eu1-N1	74.31(12)	O5-Eu1-N1	140.84(13)
O7-Eu1-O1	134.80(11)	O7-Eu1-N1	136.17(10)
O7-Eu1-O6	52.30(9)	N1-Eu1-O6	144.86(11)

Tb-DTA

Tb1-O1	2.390(4)	Tb1-O5	2.447(4)
Tb1-O2	2.235(4)	Tb1-O6	2.375(4)
Tb1-O3	2.379(4)	Tb1-N1	2.550(5)
Tb1-O4	2.455(4)	Tb1-N2	2.497(4)
O1-Tb1-O4	133.82(14)	O3-Tb1-O1	67.47(14)
O1-Tb1-O5	124.82(14)	O3-Tb1-O4	71.51(13)
O1-Tb1-N1	70.93(15)	O3-Tb1-O5	69.16(14)
O1-Tb1-N2	77.40(15)	O3-Tb1-N1	138.23(14)
O2-Tb1-O1	86.72(15)	O3-Tb1-N2	93.02(17)
O2-Tb1-O3	96.92(18)	O4-Tb1-N1	143.03(14)
O2-Tb1-O4	77.93(14)	O4-Tb1-N2	125.62(14)
O2-Tb1-O5	131.07(14)	O5-Tb1-O4	53.15(12)

O2-Tb1-O6	99.30(16)	O5-Tb1-N1	143.77(14)
O2-Tb1-N1	76.95(16)	O5-Tb1-N2	72.51(14)
O2-Tb1-N2	156.40(16)	O6-Tb1-O5	73.83(15)
O6-Tb1-O1	147.90(16)	O6-Tb1-N1	79.73(16)
O6-Tb1-O3	141.47(15)	O6-Tb1-N2	85.78(15)
O6-Tb1-O4	78.06(14)	N2-Tb1-N1	81.37(16)

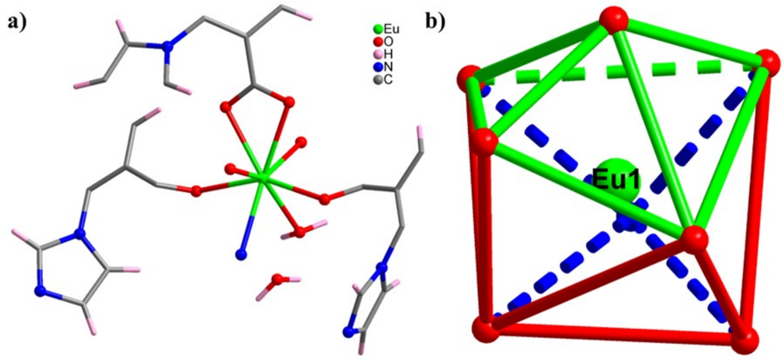

Fig. S1. a) Asymmetric structural unit of Eu-DTA; b) dodecahedral geometry of Eu^{3+} in Eu-DTA.

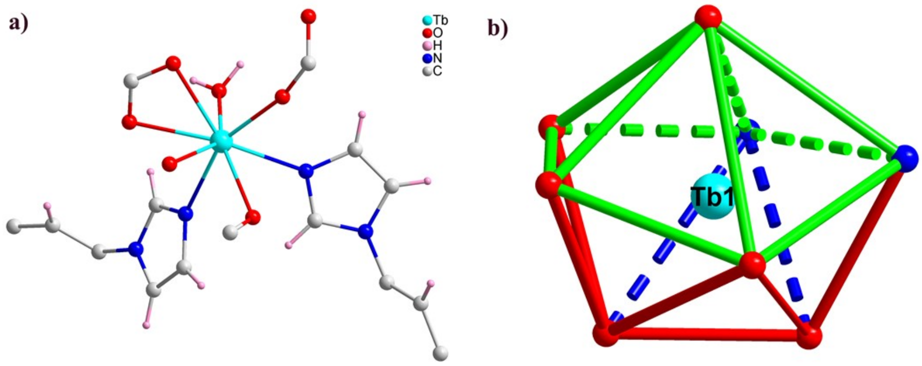

Fig. S2. a) Asymmetric structural unit of Tb-DTA; b) twisted double triangular prism geometry of Tb^{3+} in Tb-DTA.

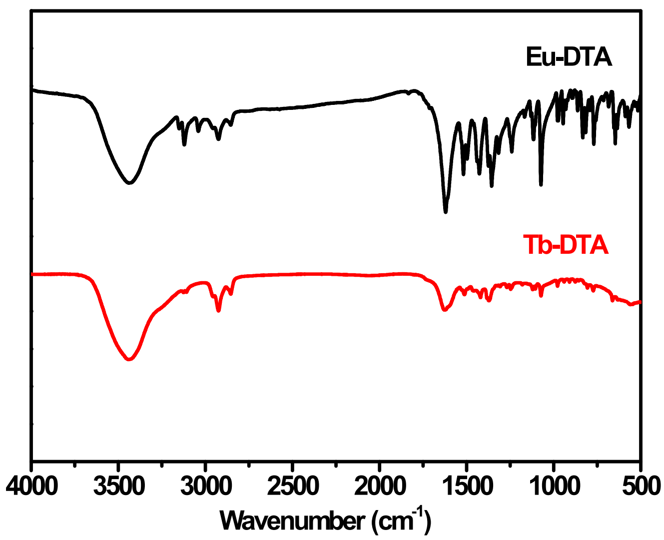

Fig. S3. IR spectra of Eu-DTA and Tb-DTA.

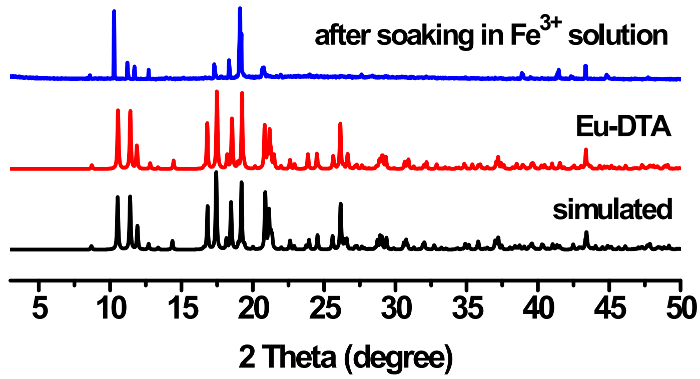

Fig. S4. Powder X-ray diffraction patterns of Eu-DTA.

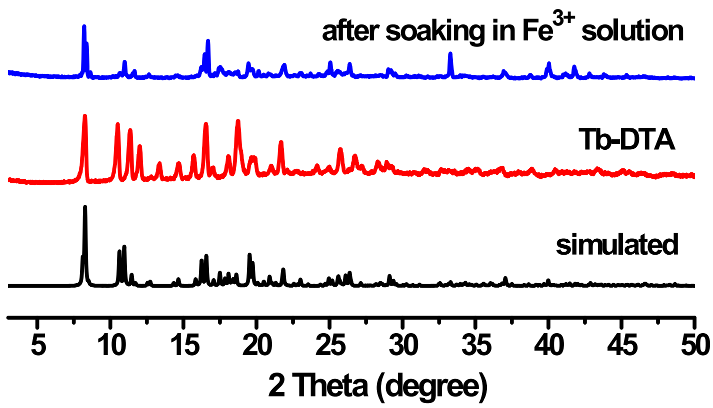

Fig. S5. Powder X-ray diffraction patterns of Tb-DTA.

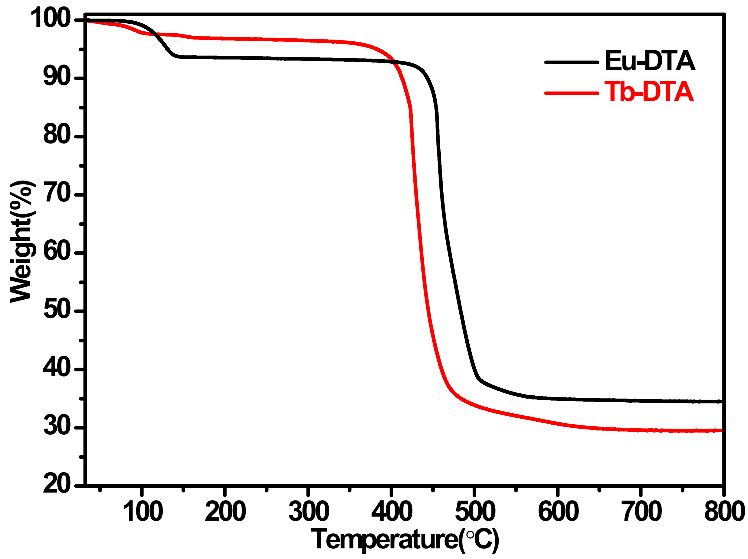

Fig. S6. TGA curves of Eu-DTA and Tb-DTA under N_2 atmosphere.

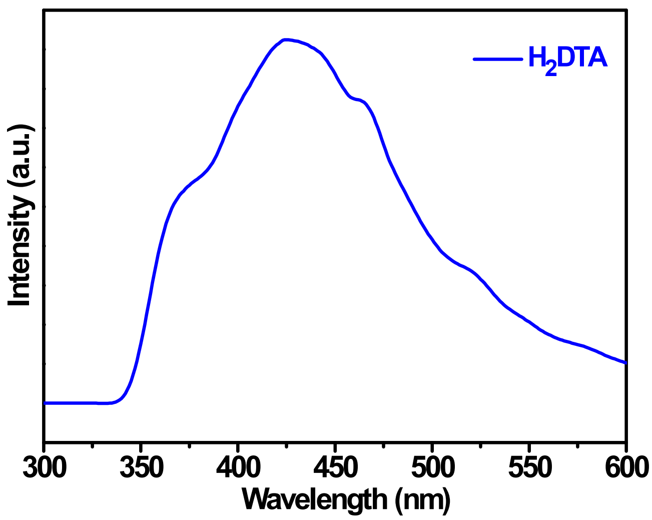

Fig. S7. Solid state emission spectra of H_2DTA.

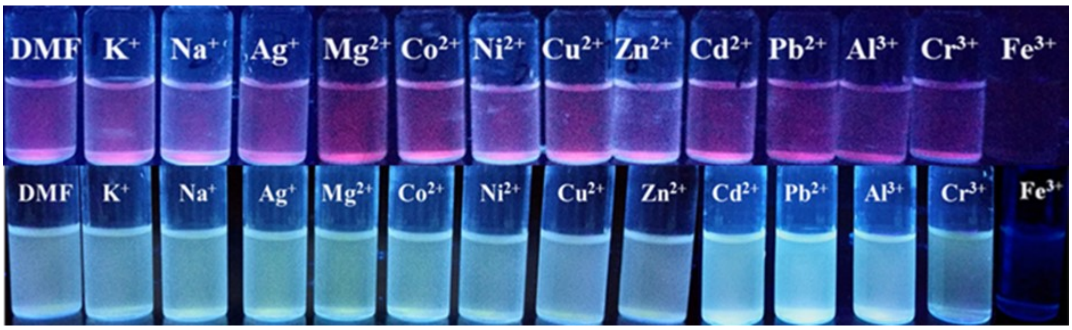

Fig. S8. Photographs showing color changes after adding metal ions under 360 nm ultraviolet light (up: Eu-DTA; down: Tb-DTA)

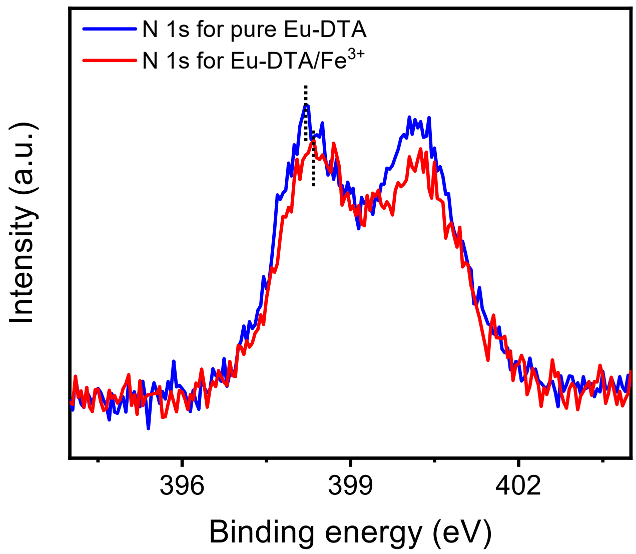

Fig. S9. N 1s spectra of the Eu-DTA (blue) and Fe^{3+}-incorporated 1 (red) activated in DMF solution of $Fe(NO_3)_3$.

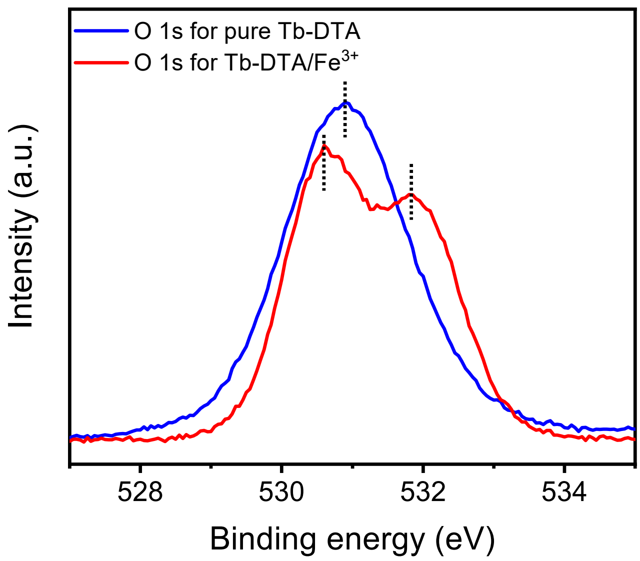

Fig. S10. O 1s spectra of the Eu-DTA (blue) and Fe^{3+}-incorporated 1 (red) activated in DMF solution of $Fe(NO_3)_3$.

Table S3. The quenching efficiencies table of selected luminescent MOFs materials for nitroaromatics.

Samples	Quenching efficiencies	Refrences
Eu-DTA	96.5%	Our work
Tb-DTA	91.5%	
$\{[Eu(L)(BPDC)_{1/2}(NO_3)]\cdot H_3O\}_n$	98.35%	ACS Appl. Mater. Interfaces
$\{[Tb(L)(BPDC)_{1/2}(NO_3)]\cdot H_3O\}_n$	99.34%	2017, 9, 1629-1634
$\{[Cd_4(HDDCP)_2(4,4'\text{-bibp})_2(H_2O)_2]\cdot 2.5(DOA)\cdot 1.5(H_2O)\}_n$	95.2%	CrystEngComm, 2020, 22,
$\{[Cd_2(HDDCP)(1,4\text{-bib})(H_2O)]\cdot H_2O\}_n$	82.3%	6927-6934
$\{[Cd_2(L)(DMA)]\cdot H_2N(Me)_2\}_n$	99%	CrystEngComm, 2018, 20, 477-486
$[(CH_3)_2NH_2]_2[In_2(H_3L)_2(OX)]\cdot 3DMF\cdot 2H_2O$	86.4%	J. Solid. State. Chem., 2021, 302, 122424.
$[Eu(HL)_3(CH_3OH)_2]_n$	90%	Cryst. Growth Des., 2017, 17, 3907-3916